ARCHIVES OF ELECTRICAL ENGINEERING VOL. 69(1), pp. 39–56 (2020)

DOI 10.24425/aee.2020.131757

The influence of pollution accumulation on coating aging of UHV line insulators with different suspension height in coal-ash polluted area

LEI LAN[1], LIN MU[1], YU WANG[1], XIAOQING YUAN[2], WEI WANG[1], ZHENGHUI LI[1]

[1] *School of Electrical Engineering and automation, Wuhan University China*

[2] *Power Dispatching and Control Center of Guizhou Power Grid Co., Ltd. China*
e-mail: yuwang@whu.edu.cn

(Received: 27.04.2019, revised: 18.09.2019)

Abstract: Room temperature vulcanized (RTV) silicone rubber is widely used to prevent pollution flashover with its excellent hydrophobicity and hydrophobicity transfer. However, RTV coatings are at the risk of deterioration and failure in heavily polluted operating environment. In this paper, RTV coated insulators with different suspension heights operating in coal ash polluted areas were sampled. Pollution degree, pollution composition and aging degree of coatings were tested. The result shows that the insoluble pollution contains $Al(OH)_3$ filler precipitated from RTV coating, which indicates the aging of the RTV coating. The top surface coating is more affected by ultraviolet and rainwater than the bottom surface resulting in more serious degradation. As the pollution degree of the lower phase insulator is heavier than that of the upper phase insulator, the erosion effect of pollution on the RTV coating is more intense. The fillers and rubber molecules of RTV continuously precipitate into the pollution layer, leading to further aging. Therefore, the overall aging degree of the lower insulator coating is more serious than that of the upper insulator coating.

Key words: aging, pollution component, pollution degree, RTV coating

1. Introduction

At present, the coal-ash pollution is aggravated, especially in the districts where the heavy industry is developing rapidly, which makes the external insulation faced with a more serious

© 2020. The Author(s). This is an open-access article distributed under the terms of the Creative Commons Attribution-NonCommercial-NoDerivatives License (CC BY-NC-ND 4.0, https://creativecommons.org/licenses/by-nc-nd/4.0/), which permits use, distribution, and reproduction in any medium, provided that the Article is properly cited, the use is non-commercial, and no modifications or adaptations are made.

www.czasopisma.pan.pl PAN POLSKA AKADEMIA NAUK www.journals.pan.pl

pollution flashover problem. The study of pollution degree and component is of great engineering significance for guiding the maintenance of external insulation [1, 2]. However, the study on pollution degree and component of coal-ash pollution is relatively rare.

RTV coating has been widely used on outdoor insulation to prevent pollution flashover with its excellent hydrophobicity and hydrophobicity transfer. However, as an organic polymer, the RTV also has the disadvantage of deterioration failure. The aging characteristics of the RTV under environmental stresses have become a research hotspot. Ultraviolet, rainwater, air oxidation will accelerate the aging of RTV coatings [3, 4]. The pollution characteristics also has a great influence on the aging degree of coatings.

Gao [5] studied pollution characteristics and hydrophobicity of RTV-coated insulators after field aging in heavily contaminated environments. Hillborg [6] studied the hydrophobicity, composition and morphology of the pollution layer on the surface of aged silicone rubber. The pollution severity test of RTV coated insulators was performed by Pylarinos [7]. But there is a lack of intensive study on the aging of coatings. Gubanski [8] studied the hydrophobicity and the component of RTV coating after natural aging. The investigation detected the presence of siloxanes and silica on the naturally aged RTV coating surface. The experiments of hydrophobicity and adhesion property on RTV coated insulators was conducted by Jia [9]. The research results showed that contamination on the surface of RTV plays a significant role in the hydrophobicity maintenance and the environmental stresses may have great impacts on adhesion property of RTV coating. Cherney [10] assessed the performance of field aged RTV coatings compared to accelerated aging coatings. The result showed a similar loss of low molecular weight substances. However, there are few studies on the aging of coatings with the analysis of pollution level and pollution components.

In this paper, equivalent salt density (ESDD) and non-soluble deposit density (NSDD), ion composition, Energy Dispersive Spectrum (EDS) and an X-ray Diffraction (XRD) test were conducted to study the pollution degree and pollution component of insulators with different suspension height. Hydrophobicity, Attenuated total reflection Fourier transformed infrared spectrum (ATR-FTIR), X-ray photoelectron spectrum (XPS) and Thermo gravimetric analysis (TGA) tests were conducted to study the aging characteristics of RTV coatings with the influence of coal-ash pollution. The aging characteristics of RTV coatings affected by coal-ash pollution are acquired.

2. Insulator samples

The insulators were collected from the tower of a 500 kV UHV transmission line in Anhui, China in December 2017. The sampling tower is 2 kilometers away from large thermal power stations that use a mixture of brown and hard coal. A three-phase line of the tower is arranged in upper and lower form. To avoid the influence of electric field on pollution accumulation and coating aging, the insulator at the low voltage end of both the upper phase and lower phase were collected. The two insulators sampled are the first insulators in the insulator string. The insulator which is of the glass type (FC300/195) with RTV coating (RTV-I) has been in service for 7 years. The sketch diagram of the insulator is shown as Figure 1.

The label of insulators and their surfaces are shown as Table 1.

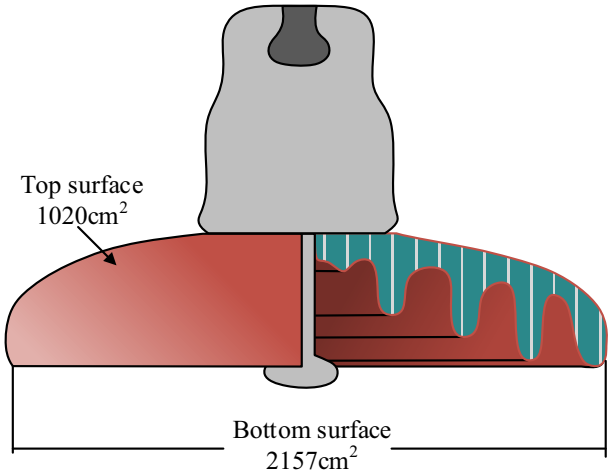

Fig. 1. The sketch diagram of the FC300/195 type with RTV coating

Table 1. The label of insulators and their surfaces

Sample	Label	Height/m	Surface	Label
Upper phase insulator	1#	200	Upper phase	Ut
			Lower phase	Ub
Lower phase insulator	2#	170	Lower phase	Lt
			Lower phase	Lb

3. Experiment setup

3.1. Pollution degree and pollution component

The ESDD and NSDD methods directly provide the content of soluble and insoluble pollution, which is a general pollution degree test [11]. Referring to the standard IEC/TS 60815-1 [12], the insulator surface was scrubbed by degreased cotton wetted by deionized water. The pollution of the top and bottom surface was collected separately. The pollution and degreased cotton of each sample were dissolved with 300 ml deionized water. In order to dissolve the pollution as fully as possible, the degreased cotton was extruded and the solution was stirred with a glass rod.

The conductivity, temperature and volume of the solution were measured. The conductivity was converted to the value at 20°C [12].

$$\sigma_{20} = \sigma_t \left[1 - b(t - 20)\right]. \tag{1}$$

Among which, b is the temperature related coefficient.

$$\sigma = -3.2 \times 10^{-8} t^3 + 1.032 \times 10^{-5} t^2 - 8.272 \times 10^{-4} t + 3.544 \times 10^{-2}. \tag{2}$$

www.czasopisma.pan.pl PAN POLSKA AKADEMIA NAUK www.journals.pan.pl

Then, the S_a (salinity, kg/m^3) can be calculated according to conductivity as the expression below [12].

$$S_a = (5.7\sigma_{20})^{1.03}. \tag{3}$$

The ESDD can be obtained by calculating the salt content of the unit area [12].

$$\text{ESDD} = \frac{S_a \times V}{A}. \tag{4}$$

Among which, V represents the solution volume, A represents the surface area of the tested insulator.

Quantitative filter paper was dried at 60°C for 2 hours and weighed with electronic balance. The pollution suspension was filtered and the filtration residue with the filter paper was dried at 60°C for 6 hours and weighed. The net weight of the insoluble pollution was obtained by subtracting the weight of the paper. NSDD can be obtained by calculating the net mass of an unit area [12].

$$\text{NSDD} = \frac{m \times m_p}{A}. \tag{5}$$

Among which, m represents the total mass of the insoluble pollution and filter paper after drying. m_p represents the mass of the dried filter paper.

Inductively Coupled Plasma Atomic Emission Spectrometry (ICP-AES) provides high precision for an element composition test, it has been widely applied [13]. Ion Chromatography (IC) has advantages in detecting the ionic species in water and is considered as the standard analytical technique [14].

After the ESDD and NSDD test, 100 ml of the filtrate was tested by ICP-AES (type of instrument: IRIS Intrepid II XSP) and IC (type of instrument: ICS2500) to analyze the species and concentration of cations and anions of soluble pollution respectively. EDS (type of instrument: QUANTA 200) was adopted to analyze element composition of insoluble pollution. 100 mg of sediment powder was dried and glued to the sample holder. The surface of the specimen was scanned by an electron beam at a selected point. The acquisition time of secondary electrons of one point analysis is 60 s. According to the spectrum of secondary electrons, the types and contents of elements can be determined. XRD (type of instrument: XPert Pro) was adopted to analyze crystal composition of the insoluble pollution. 100 mg of sediment was dried and scanned at a wide angle of 10°–70° with a resolution of 0.1°.

3.2. Appearance and hydrophobicity of RTV coating

After the pollution collection was completed, the samples were manually inspected to find fading and peeling off of the RTV coating.

According to the shape of water drops and the proportions of the wetted area of the coating, the surface is divided into seven hydrophobic classes. Hydrophobicity of HC1 surface is the best, while HC7 surface is hydrophilic [15]. The insulators were placed at room temperature for 72 hours until the coating got completely dry. Water mist was sprayed on the surface of the coating at a distance of 25 cm for 20 seconds. The surface of the coating was observed to assess hydrophobicity.

www.czasopisma.pan.pl PAN POLSKA AKADEMIA NAUK www.journals.pan.pl

As aging of coatings of some areas is uneven, the coating samples with better adhesion and uniformity of the top surface and bottom surface were taken, respectively, as typical aged coatings. A contact angle tester (type: SL150E) was employed to accurately evaluate the hydrophobicity of the coating. A 1 cm × 1 cm coating was pasted on the flat glass. A deionized water drop of 4 μL was dripped to the surface of the sample. The shape of the water drop was captured by an industrial camera 5 seconds later. The static contact angle was calculated based on the Young-Laplace method.

3.3. Aging characteristics of RTV coating

The aging degree of RTV coating can be assessed by the change of Si-C and Si-O functional groups [16]. ATR-FTIR (type of instrument: Nicolet5700) was adopted to measure the intensity of characteristic infrared absorption peaks indicating the content of functional groups. The 1 cm× 1 cm coating was cleaned with ethanol and dried at 60°C for 1 hour. The sample was scanned in the infrared frequency range of 400 cm^{-1} to 4 000 cm^{-1} at a resolution of 0.5 cm^{-1}. The analytical depth of FTIR is 1–10 um.

The variation of element content and chemical structure of the surface of coating is related to aging. The 1 cm × 1 cm coating sample was cleaned and dried. XPS (type of instrument: ESCALAB250Xi) was employed to evaluate the content of C, O, Si, Al elements and chemical structure of Si 2p on the coating surface in the range of nanometer depth.

TGA obtains content of RTV component by weight loss during heating process [17]. The coating samples were cleaned and dried. A 5 mg sample was taken and heated from room temperature to 400°C at a rate of 15°C/min in nitrogen atmosphere with a TG analyzer (Hitachi 7300), respectively.

4. Test result and discussion

4.1. ESDD and NSDD

ESDD equates the amount of NaCl required to yield the same conductivity as the contaminant when dissolved in the same volume of water. NSDD is used to quantify the amount of non-soluble residue on contaminated insulators [11]. The ESDD and NSDD of insulator surfaces are shown in Figure 2.

The ratio of ESDD and NSDD between the bottom and top surfaces was obtained, respectively, to study the inhomogeneity of pollution accumulation of the top and bottom surfaces of the insulator. In order to study the relative content variety of soluble contaminants and insoluble pollution of the insulator surfaces, the ratio of NSDD to ESDD on insulator' surfaces was calculated as shown in Table 2.

It can be seen from the result that the pollution of the 2# insulator is more severe than that of the 1# insulator. The main reason is that the concentration of dust particles from the ground decreases with the increase of height and the effect of wind and rain cleaning the upper phase is more intense. There is much more pollution on the bottom surface than on the top surface, which is mainly because the top surface is significantly washed by wind and rain.

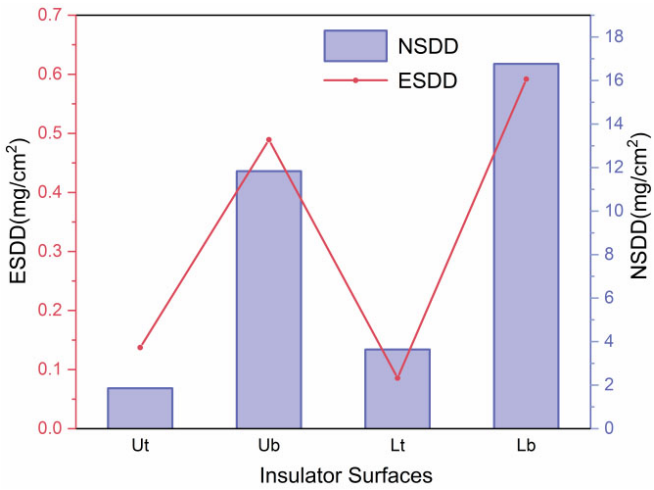

Fig. 2. The ESDD and NSDD of insulator surfaces

Table 2. Inhomogeneity and ratio of NSDD to ESDD

Insulators		**1#**	**2#**
Inhomogeneity	ESDD	3.57	6.91
	NSDD	6.39	4.61
NSDD/ESDD	Top surface	13.50	42.47
	Bottom surface	24.19	28.33

The pollution on the RTV coated insulator is heavier than that of the glass insulators and the inhomogeneity of pollution between the top and bottom surfaces is smaller than that of the glass insulators [18]. This may be due to the fact that the migration of an RTV bulk molecule makes the pollution layer hydrophobic. In heavy pollution severity, the pollution layer is compact and not easy to be cleaned. According to the ratio of NSDD to ESDD, it can be seen that the content of the insoluble substance in the sampled pollution is higher than that of ordinary pollution [19].

4.2. Ion composition of soluble pollution

The composition of soluble pollution has a great influence on the flashover resistance of insulators [20]. The concentration of cations in the filtrate is shown in Table 3, the relative proportion of mass fraction of the major cations is shown in Figure 3. The main ions are selected for analysis ignoring other ions with minor content.

It can be seen from the result that most cations in the filtrate are Ca^{2+} and Na^{+}. It indicates that the main components of soluble pollution are calcium and sodium salts, which is conformed to a typical insulator pollution component of inland areas [21]. The contents of Ca^{2+}, Na^{+}, K^{+} and Mg^{2+} in the pollution of the 2# insulator are higher than that of the 1# insulator. It indicates that

Table 3. The concentration of cations in filtrate (mg/L)

Cations	Ut	Ub	Lt	Lb
Al^{3+}	0.28	0.45	0.1	2.65
Ca^{2+}	51.12	938.5	83.85	1097
Fe^{3+}	0.063	0.061	0.017	0.13
K^{+}	1.72	52.07	3.21	84.75
Mg^{2+}	1.77	94.56	3.01	161.9
Na^{+}	5.87	143.7	8.2	228.9

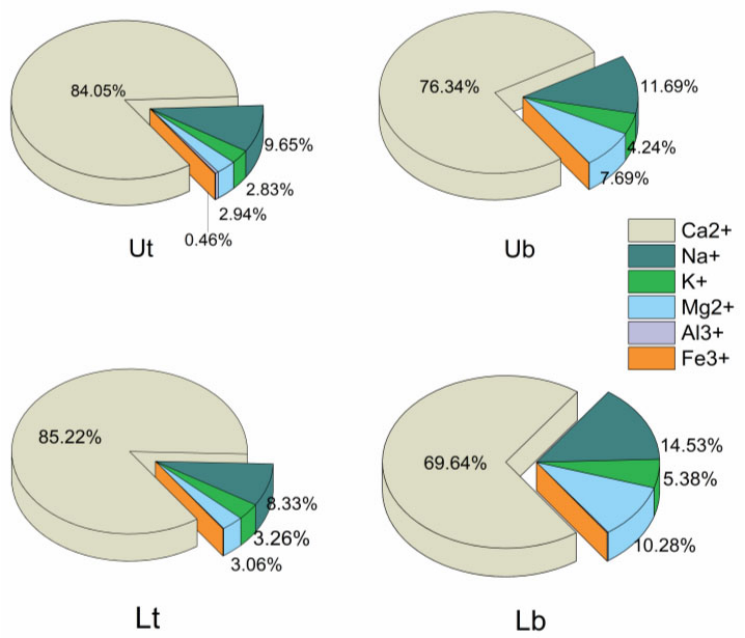

Fig. 3. The relative proportion of mass fraction of the major cations

these soluble pollutions mainly come from road dust causing an insulator with lower suspension position polluted more heavily. The pollution content on the top surface of the insulator is much less than that on the bottom surface. The reason is that soluble pollution on a top surface can easily be dissolved and washed away by rain, while a bottom surface is rarely washed by rain.

The concentration of anions in the filtrate is shown in Table 4, the relative proportion of the mass fraction of the major cations is shown in Figure 4. It can be seen from the result that the anions in the pollution filtrate of the bottom surface are mainly SO_4^{2-} and NO_3^-. The top surface pollution filtrate mainly contains SO_4^{2-} with little NO_3^-. The concentration of pollution anions of the bottom surface is much higher than that of the top surface. The pollution on the top surface

can be washed away by rain more easily. Nitrate is especially soluble by rainwater, so the nitrate content of the top surface pollution is very low. The concentration of pollution anions of the 2# insulator is also higher than that of the 1# insulator. It indicates that the insulator with the lower suspension position is polluted more heavily. SO_4^{2-} and NO_3^- mainly come from acid rain, among which SO_4^{2-} is formed by combustion of sulfur in coal.

Table 4. The concentration of anions in filtrate (mg/L)

Anions	**Ut**	**Ub**	**Lt**	**Lb**
SO_4^{2-}	147.32	1467.57	258.65	1481.86
NO_3^-	< 0.03	1243.75	< 0.03	2000.93
Cl^-	3.88	185.32	6.16	319.41
F^-	2.50	13.21	0.51	10.96

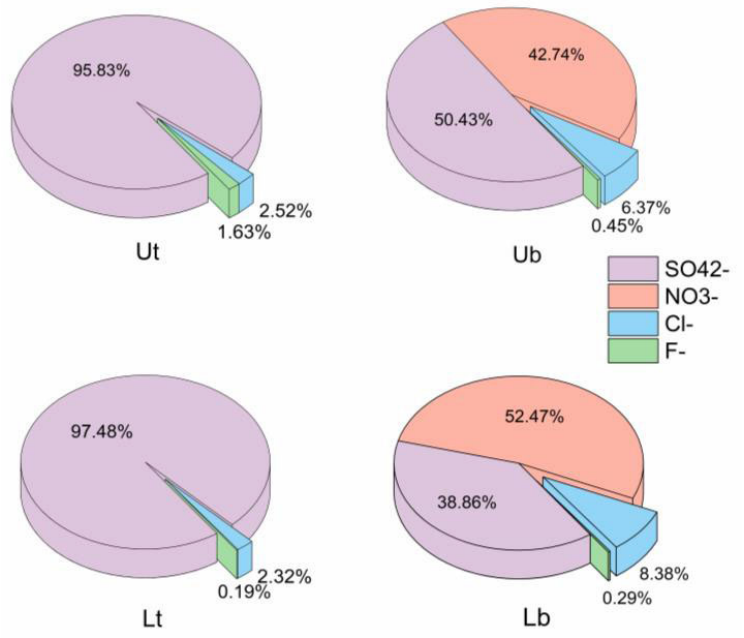

Fig. 4. The relative proportion of mass fraction of the major anions

As the influence of monovalent alkali metal salt on pollution flashover voltage is greater, monovalent salt was paired first. Ion pairing is then performed according to the solubility [22]. According to the composition of an anion and cation, it can be determined that soluble pollutions of a top surface are mainly NaCl, Na_2SO_4 and $CaSO_4$. Soluble pollutions of a bottom surface are mainly NaCl, KNO_3, $Mg(NO_3)_2$, $Ca(NO_3)_2$ and $CaSO_4$.

4.3. Element composition of insoluble pollution

EDS has been proved to be a suitable method to investigate elemental composition of pollution [23]. Energy dispersive spectrum of the insoluble pollution samples is shown in Figure 5. The element content can be indicated by spectral peak height. The mass percentage of the detected elements is shown in Table 5.

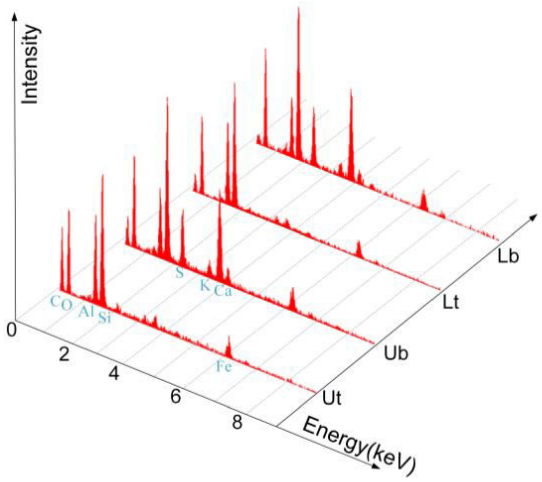

Fig. 5. Energy spectrum of EDS test

Table 5. The element mass percentage of pollutions (%)

Element	Ut	Ub	Lt	Lb
C	45.93	28.48	30.77	17.02
O	35.56	41.27	40.58	45.02
Na	0.24	0.31	0.38	0.77
Al	5.31	4.69	9.02	5.22
Si	8.91	11.21	13.70	13.69
S	0.48	3.68	0.55	4.97
K	0.44	0.94	0.65	1.19
Ca	0.78	6.32	0.93	8.59
Fe	2.38	3.10	3.43	3.53

It can be seen from the result that the content of Ca and S in the insoluble pollution of the top surface is much lower than that of the bottom surface. The reason is that $CaSO_4$, which is slightly soluble in water, can be dissolved and washed away by a large amount of rain water. The element contents of the 2# insulator are higher than that of the 1# insulator except carbon. Insoluble carbon may come from the coal ash emitted by chimneys of thermal power plants. It settles down from

www.czasopisma.pan.pl PAN POLSKA AKADEMIA NAUK www.journals.pan.pl

a high position and can be adsorbed and deposited on an insulator surface [21]. The insoluble substance containing elements other than C mainly come from the ground and the coating. The sources of the Si element in insoluble pollution include RTV filler white carbon black and silica in road dust. The Al element mainly comes from precipitation of RTV filler with ATH.

4.4. Crystal component of insoluble pollution

The peak position of the diffraction spectrum is determined by the structure and type of the crystal. By comparing the peak position with the standard diffraction spectrum, the crystal composition of the samples is determined. The XRD patterns are shown in Figure 6. The black curve is the spectrum of insoluble pollution samples. The color vertical lines are the standard spectrums of four most probable crystal compositions.

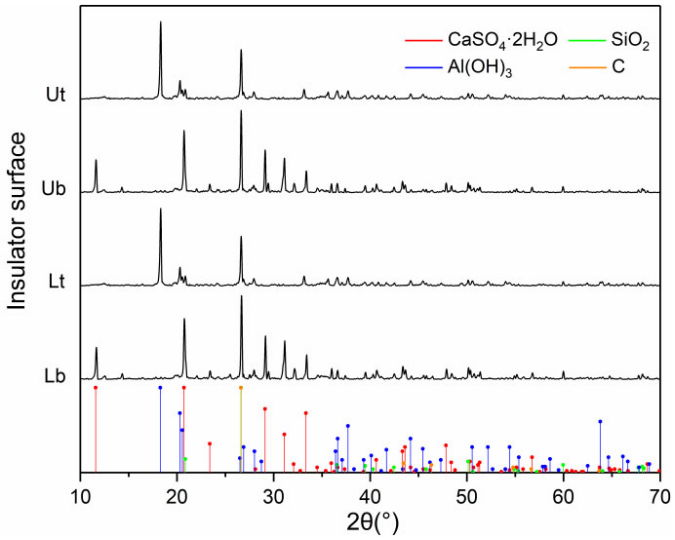

Fig. 6. The XRD patterns

It can be seen from the result that there are mainly narrow and spiky peaks in the patterns indicating that the crystallinity of the sample is high [24]. The content of $CaSO_4 \cdot 2H_2O$ of the bottom surface pollution is higher than that of the upper surface. The detected silica comes from road dust due to the fact that white carbon black is not crystal. All the pollution samples contain a certain amount of SiO_2. The carbon in insoluble pollution is from coal ash according to the crystal phase. There is a characteristic diffraction peak of $Al(OH)_3$ in XRD patterns. The peak heights of the main diffraction peak of $Al(OH)_3$ of Ut, Ub, Lt and Lb are 3 861, 101, 4 148 and 109, respectively. The $Al(OH)_3$ crystal is the ATH filler precipitated from the RTV coating, which indicates the aging of the coating. Therefore, it can be inferred from the result that the aging of the RTV coating of the top surface is more serious than that of the bottom surface. The overall aging of the RTV coating of the 2# insulator is more serious than that of the 1# insulator. The further study was performed to figure out the structure and property change of the RTV coating samples.

4.5. Appearance and hydrophobicity

Hydrophobicity, color fading and peeling off of RTV coating can reflect the aging degree and has great influence on insulation characteristics. The insulators attached with water drops are shown in Figure 7.

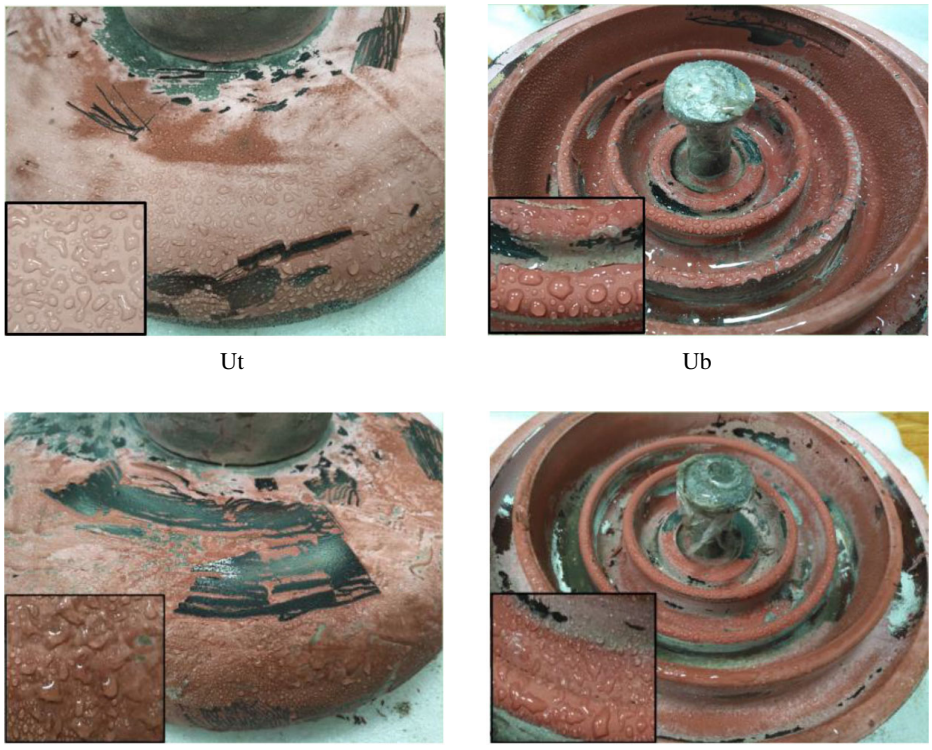

Ut Ub

Lt Lb

Fig. 7. The insulators attached with water drops

It can be seen from the size and distribution of the water drops that the hydrophobicity of the bottom surface is better than that of the top surface. The overall hydrophobicity of the 1# insulators is better than that of 2#.

Referring to the standard IET/TS 62073, the hydrophobicity class of the coating surface is evaluated. Ut is HC3, Ub is HC2, Lt is HC3~HC5, Lb is HC3. It can be seen from the appearance of the coating that peeling off phenomena of 2# is more serious, while color fading of the upper surface of 1# is more obvious. The grooves of the bottom surface accumulate more pollution and there is a large area of coating peeling off. The coating peeling off of Lt is more serious than that of Ut. The reason may be that the NSDD of Lt is higher than that of Ut. Contaminants have erosion effect on RTV coatings. The continuous precipitation of fillers makes the coating porous and the adhesion of coating decreases. The color fading and peeling off is a sign of aging of the RTV coating.

The water droplets in the static contact angel test are shown in Figure 8. It can be seen from the result that the hydrophobicity of the top surface coating is relatively poorer than that of the bottom surface. The overall hydrophobicity of 1# is better than that of 2#. After seven years of operation, the hydrophobicity of the RTV coating is lower than that of the new one, but it still has good hydrophobicity. It shows that the coating can reach the 8-year service life specified in the standard DL/T627-2012, but it's necessary to recoat the insulators to maintain safe operation.

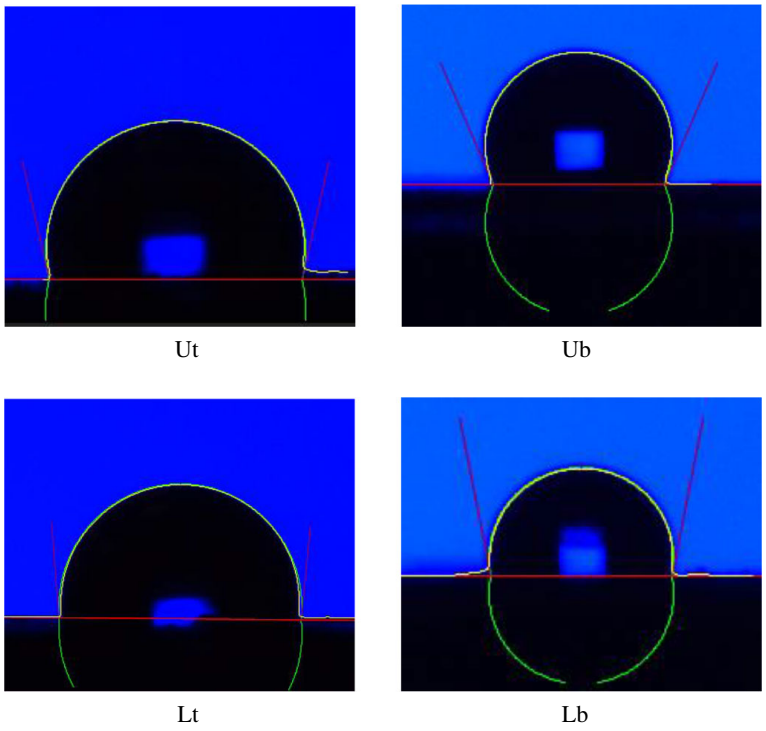

Ut Ub

Lt Lb

Fig. 8. The water droplets in the static contact angle test

4.6. ATR-FTIR

$Si(CH_3)_2$ and $Si\text{-}CH_3$ are side chains and major organic functional groups of polysiloxane molecules, which have great effect on the hydrophobicity of RTV. The absorption peak caused by vibration of $Si(CH_3)_2$ and $Si\text{-}CH_3$ are located at 790–840 cm^{-1} and 1 240–1 280 cm^{-1}, respectively. SiOSi is the main chain and cross linkage of polysiloxane, whose integrity can characterize aging degree of RTV. The absorption peak caused by symmetric stretching of SiOSi is located at 1 000–1 100 cm^{-1}. The FTIR spectrum of the coating sample is shown in Figure 9.

The functional group content can be reflected by absorption peak height. The $Si(CH_3)_2$ and $Si\text{-}CH_3$ are the side chains of siloxane. The side chains break down from the main chain with the effect of aging factors. The result indicates that the side chain fracture of the top surface is more serious than that of the bottom surface and the side chain fracture of the 2# insulator is more serious than that of the 1# insulator. Methyl groups on the side chains are non-polar

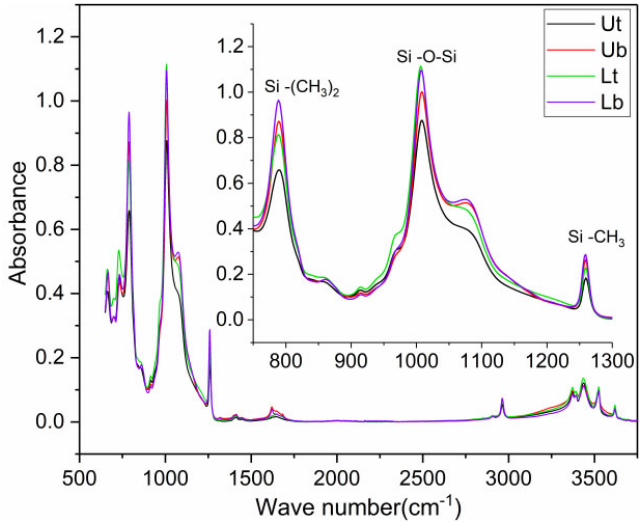

Fig. 9. The FTIR spectrum of the coating sample

and surface-oriented, preventing water molecules from approaching hydrophilic backbones. The lower the content of the side chains, the poorer the hydrophobicity of the coatings. Therefore, the result of the side chain content conforms to the result of the hydrophobicity test result in section 4.5.

The O-H (3 200–3 700 cm^{-1}) content of the top surface coating is higher than the bottom surface coating, which shows that oxidation and hydrolysis of the top surface is more intense. The Si-O-Si absorption peak changes from a double peak to a single peak structure, which is a sign of transition from a long chain to a cross-linked network. The main chain fracture of the 2# insulators is more serious than that of the 1# insulators. It indicates that the aging degree of the 2# insulator is more serious than that of the 1# insulator. The change of the cross linkages of polysiloxane and the bonding state of Si can be depicted by a XPS test in detail.

4.7. XPS

The relative content of C, O, Si and Al obtained by XPS can reflect the content changes of inorganic fillers and rubber bulk on the RTV surface. The atomic composition is shown in Table 6.

Table 6. Atomic composition of RTV coating

Samples	C(%)	O(%)	Si(%)	Al(%)
Ut	44.37	29.42	24.95	1.26
Ub	46.69	27	25.89	0.43
Lt	43.67	30.94	24.11	1.27
Lb	44.97	30.28	23.57	1.18

www.czasopisma.pan.pl PAN POLSKA AKADEMIA NAUK www.journals.pan.pl

The content of a carbon atom of the top surface coating is lower than that of the bottom surface and an oxygen atom of the top surface coating is higher than that of the bottom surface. The main reason might be that the organic functional groups of the top surface RTV coating are oxidized more seriously under the effect of air and rainwater. The Si-CH_3 bond is fractured and reacts with other free radicals releasing methane. The content of an oxygen atom increases with the introduction of hydroxyl groups in oxidation and hydrolysis reactions. Therefore, the hydrophobicity of the top surface coating is worse than the bottom surface coating, which conforms to the results of the hydrophobicity tests. The relative content of aluminum atoms of the top surface coating is higher than that of the bottom surface, which is considered to be related to the precipitation of the ATH filler combined with the test result of the composition of insoluble pollution. The fillers are usually covered by siloxanes. It shows that the more serious the aging of the coating, the more the filler precipitates. With the loss of the ATH filler, the leakage current and high temperature resistance properties of RTV declined.

Silicon atoms have different binding energies when connected with the different number of oxygen atoms [25]. The Si 2p spectrum is resolved and fitted by four components, with an increase in binding energy for the replacement of each methyl group by an additional oxygen atom [26]. There are mainly three chemical structures including $Si(-O)_2$, $Si(-O)_3$ and $Si(-O)_4$, among which the $Si(-O)_4$ is silica like structure [27]. Due to the different experimental conditions, the peak position can be different from standard binding energy. The peak position of C1 s was used to adjust the difference [28]. The resolving and fitting result of Si 2p spectrum is shown in Figure 10.

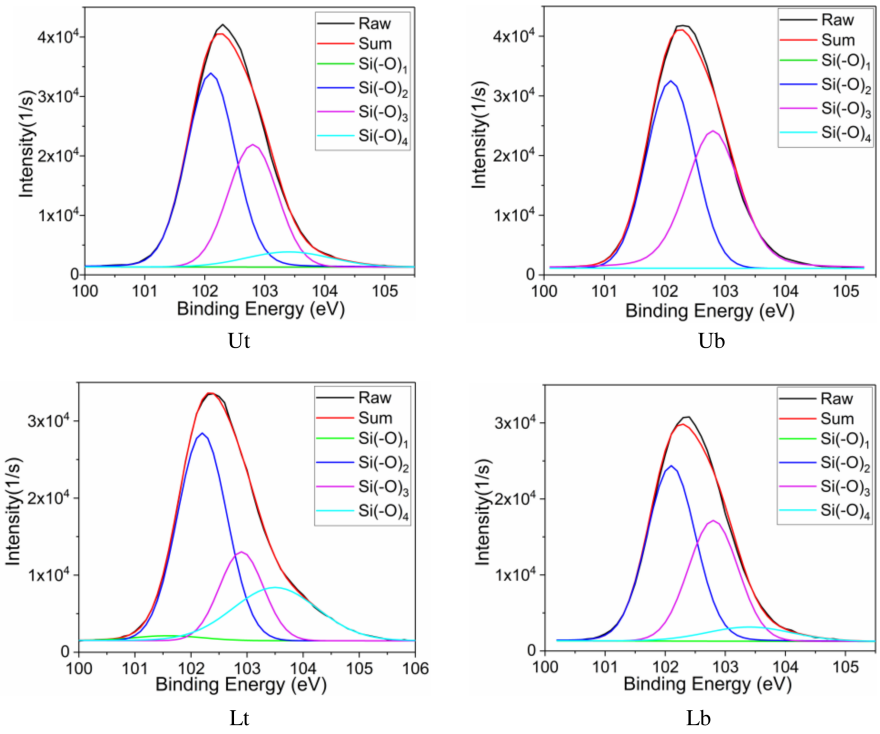

Fig. 10. The resolving and fitting result of Si 2p spectrum

The original spectrum is represented by black lines in the figure. The red line is the sum of the peaks fitting the original spectrum. As can be seen from the result, the ratio of the peak area of $Si(-O)_4$ of the top surface is larger than that of the bottom surface, while the ratio of the peak area of $Si(-O)_3$ of the top surface is smaller than that of the bottom surface. With the aging of RTV, the $Si(-O)_3$ gradually change into $Si(-O)_4$. This is due to the oxidation of the side chain group as well as the crosslinking reaction between polydimethylsiloxane chains. With the increase of crosslinking density, the hardness of the coating increases and the adhesion decreases. The precipitation of white carbon black filler may also increase the content of $Si(-O)_4$. The precipitation of filler can increase porosity, reduce the mechanical strength, accelerate the aging of the coating.

4.8. TG analysis

The TG analysis can be applied to the study of thermal stability and thermal degradation mechanism of RTV [29]. High temperature resistant filler ATH in RTV decomposes between 250°C and 300°C losing water. The content of the ATH filler in RTV can be estimated according to the weight reduction in the above temperature range. The TG curves of the RTV coating samples are shown in Figure 11.

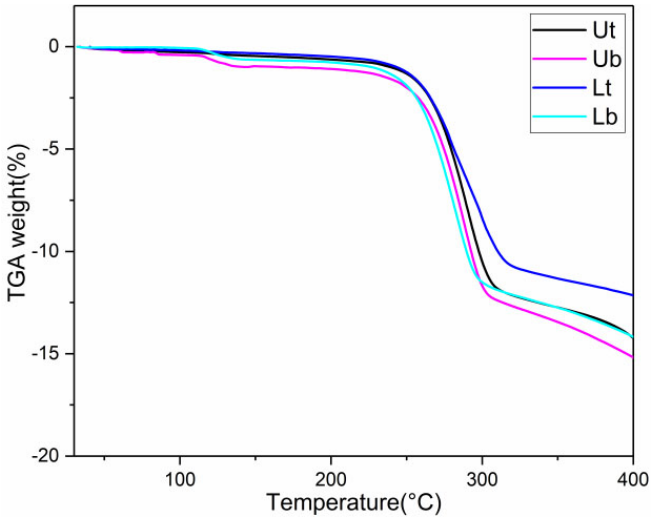

Fig. 11. The TG curves of RTV coating samples

It can be seen from the result that in the range of 250°C to 300°C, the weight losses of Ut, Ub, Lt and Lb samples are 9.19%, 9.69%, 7.14% and 9.62%, respectively, which indicates that the content of the ATH filler of the top surface coating is lower than that of the bottom surface coating, the overall content of the ATH filler of the 2# insulator is lower than that of the 1# insulator. The change trend of the ATH filler content in the coating is opposite to that in pollution. The main reason may be that ATH fillers precipitate into the pollution layer during the aging process of RTV [9].

www.czasopisma.pan.pl PAN POLSKA AKADEMIA NAUK www.journals.pan.pl

5. Conclusion

The insoluble pollution contains relatively large amount of carbon, silica and $Al(OH)_3$. The carbon in insoluble pollution mainly comes from coal ash emitted by thermal power plants. $Al(OH)_3$ is mainly contributed by precipitation of the coating filler. Soluble pollutions of the top surface are mainly NaCl, Na_2SO_4 and $CaSO_4$. Soluble pollutions of the bottom surface are mainly NaCl, KNO_3, $Mg(NO_3)_2$, $Ca(NO_3)_2$ and $CaSO_4$.

With the effect of ultraviolet and rainwater, the oxidative hydrolysis reaction occurred more intensely on the top surface. The RTV functional group content and silicon atom chemical structure show that the aging degree of the top surface coating is more serious than the bottom surface coating.

The closer to the ground, the higher the concentration of pollution particles. Thus, the pollution degree of the 2# insulator is heavier than that of the 1# insulator.

The aging degree of the 2# insulator coating is more serious than that of the 1# insulator according to the RTV functional group content and silicon atom chemical structure.

While the content of the ATH filler of the 2# insulator coating is lower than that of the 1# insulator coating, the Al content on the surface of the 2# insulator coating is higher than that of 1#, the content of ATH crystals in the pollution of the 2# insulator is higher than that of the 1# insulator indicating that the ATH filler of the coating will precipitate into the pollution layer during aging process, which could increase the porosity of the coating and lead to further aging.

The results indicate that the heavier the pollution degree, the stronger the erosion of pollution on RTV coating, the faster the loss of fillers and rubber molecules, and the more serious the aging degree of RTV coating.

After seven years of operation, the RTV coating still has good hydrophobicity. Thus, the coating can meet the required service life. The hydrophobicity of the top surface coating decreases obviously and bottom surface coating peels off severely. It is necessary to recoat the insulators with RTV to maintain safe operation.

References

[1] Ramos G., Campillo M.T., Naito K., *Study on the characteristics of various conductive contaminants accumulated on high voltage insulators*, IEEE Transactions on Power Delivery, vol. 8, no. 4, pp. 1842–1850 (1993).

[2] Briancin J. *et al.*, *Environmental Pollution Monitoring on High-Voltage Insulators*, Inzynieria Mineralna-Journal of the Polish Mineral Engineering Society, no. 1, pp. 111–114 (2018).

[3] Allen B., Bleszynski M., Kumosa M., Willis E., *Investigation into the effects of environmental stresses on RTV-1 silicone-based caulk materials*, IEEE Transactions on Dielectrics and Electrical Insulation, vol. 22, no. 5, pp. 2978–2986 (2015).

[4] Bleszynski M., Kumosa M., *Silicone rubber RTV-1 aging in the presence of aqueous salt*, IEEE Transactions on Dielectrics and Electrical Insulation, vol. 23, no. 5, pp. 2822–2829 (2016).

[5] Gao H., Jia Z., Guan Z., Wang L., Zhu K., *Investigation on Field-Aged RTV-Coated Insulators Used in Heavily Contaminated Areas*, IEEE Transactions on Power Delivery, vol. 22, no. 2, pp. 1117–1124 (2007).

[6] Hillborg H., Krivda A., Schmidt L., Kornmann X., *Investigation of hydrophilic pollution layers on silicone rubber outdoor insulation*, in Electrical Insulation and Dielectric Phenomena, pp. 1–4 (2010).

www.czasopisma.pan.pl PAN POLSKA AKADEMIA NAUK www.journals.pan.pl

[7] Pylarinos D., Siderakis K., Thalassinakis E., *Comparative investigation of silicone rubber composite and room temperature vulcanized coated glass insulators installed in coastal overhead transmission lines*, IEEE Electrical Insulation Magazine, vol. 31, no. 2, pp. 23–29 (2015).

[8] Gubanski S.M., *Properties of silicone rubber housings and coatings*, IEEE Transactions on Electrical Insulation, vol. 27, no. 2, pp. 374–382 (2002).

[9] Chen C., Jia Z., Lu H., Yang Z., Li T., *Field aging investigation and filler precipitation analysis on RTV coated insulators in China*, IEEE Transactions on Dielectrics and Electrical Insulation, vol. 21, no. 6, pp. 2458–2465 (2014).

[10] Jahromi A.N., Cherney E.A., Jayaram S.H., Simon L.C., *Aging characteristics of RTV silicone rubber insulator coatings*, IEEE Transactions on Dielectrics and Electrical Insulation, vol. 15, no. 2, pp. 444–452 (2008).

[11] Wardman J., Wilson T., Bodger P., *Volcanic ash contamination: limitations of the standard ESDD method for classifying pollution severity*, IEEE Transactions on Dielectrics and Electrical Insulation, vol. 20, no. 2, pp. 414–420 (2013).

[12] *Selection and dimensioning of high-voltage insulators intended for use in polluted conditions*, IEC TS 60815 (2008).

[13] Lee H., Choi Y., Suh J., Lee S.-H., *Mapping Copper and Lead Concentrations at Abandoned Mine Areas Using Element Analysis Data from ICP-AES and Portable XRF Instruments: A Comparative Study*, International Journal of Environmental Research and Public Health, vol. 13, no. 4 (2016).

[14] Murray E. *et al.*, *Miniaturized capillary ion chromatograph with UV light-emitting diode based indirect absorbance detection for anion analysis in potable and environmental waters*, Journal of Separation Science, vol. 41, no. 16 (2018).

[15] *Guidance on the measurement of hydrophobicity of insulator surfaces*, IEC TS 62073 (2016).

[16] Amin M., Khattak A., Ali M., *Accelerated aging investigation of silicone rubber/silica composites for coating of high-voltage insulators*, Electrical Engineering, no. 1, pp. 1–14 (2016).

[17] Wang J.J., Feng L.J., Lei A.L., Yan A.J., Wang X.J., *Thermal stability and mechanical properties of room temperature vulcanized silicone rubbers*, Journal of Applied Polymer Science, vol. 125, no. 1, pp. 505–511 (2012).

[18] Wang S., Hu W., Gong J., Pan J., Xu Y., Liu H., *Natural pollution accumulation characteristics of overhead transmission line insulator strings of Zhejiang electric power grid*, Gaodianya Jishu/High Voltage Engineering, vol. 40, no. 4, pp. 1002–1009 (2014).

[19] Su Z.-Y., Liu Y.-S., *Comparison of natural contaminants accumulated on surfaces of suspension and post insulators with DC and AC stress in northern China's inland areas*, Power System Technology, vol. 28, no. 10, pp. 13–17 (2004).

[20] Jiang X., Xin L.I., Zhang D., Zhang Z., Hanxin Y.E., Maoqiang B.I., *Effect of Soluble Contamination on the AC Flashover Performance of Insulator*, High Voltage Engineering, vol. 41, no. 6, pp. 1915-1920 (2015).

[21] Gao F. *et al.*, *Analysis on contamination components of energized insulator of Hami-Zhengzhou overhead line in Henan and influence of installation height on pollution accumulation*, Dianwang Jishu/Power System Technology, vol. 39, no. 10, pp. 2923–2928 (2015).

[22] Hengzhen L.I., Gang L.I.U., Licheng L.I., *Study Status and Prospect of Natural Contamination Component on Insulator Surface*, Proceedings of the Chinese Society of Electrical Engineering, vol. 31, no. 16, pp. 128–137 (2011).

[23] Milos M., Mateja G., *Assessment of Metal Pollution Sources by SEM/EDS Analysis of Solid Particles in Snow: A Case Study of Zerjav, Slovenia*, Microscopy and Microanalysis the Official Journal of

www.czasopisma.pan.pl PAN POLSKA AKADEMIA NAUK www.journals.pan.pl

Microscopy Society of America Microbeam Analysis Society Microscopical Society of Canada, vol. 19, no. 6, pp. 1606–1619 (2013).

[24] Bhattacharjee A., Mandal H., Roy M., Chini T.K., *A preliminary study on the nature of particulate matters in vehicle fuel wastes*, Environmental Monitoring and Assessment, journal article, vol. 176, no. 1, pp. 473–481 (2011).

[25] O'Hare L.A., Hynes A., Alexander M.R., *A methodology for curve-fitting of the XPS Si 2p core level from thin siloxane coatings*, Surface and Interface Analysis, vol. 39, no. 12-13, pp. 926-936 (2007).

[26] Ward L.J., Schofield W.C.E., Badyal J.P.S., Goodwin A.J., Merlin P.J., *Atmospheric Pressure Glow Discharge Deposition of Polysiloxane and SiO_x Films*, Langmuir, vol. 19, no. 19, pp. 2110-2114 (2003).

[27] Bodas D., Rauch J.-Y., Khan-Malek C., *Surface modification and aging studies of addition-curing silicone rubbers by oxygen plasma*, European Polymer Journal, vol. 44, no. 7, pp. 2130–2139 (2008).

[28] O'Hare L.-A., Parbhoo B., Leadley S.R., *Development of a methodology for XPS curve-fitting of the Si 2p core level of siloxane materials*, Surface and Interface Analysis, vol. 36, no. 10, pp. 1427–1434 (2004).

[29] He C. *et al.*, *How the Crosslinking Agent Influences the Thermal Stability of RTV Phenyl Silicone Rubber*, Materials, vol. 12, no. 1 (2019).